Article

Neuron

Functional Brain Networks Are Dominated by Stable Group and Individual Factors, Not Cognitive or Daily Variation

Graphical Abstract

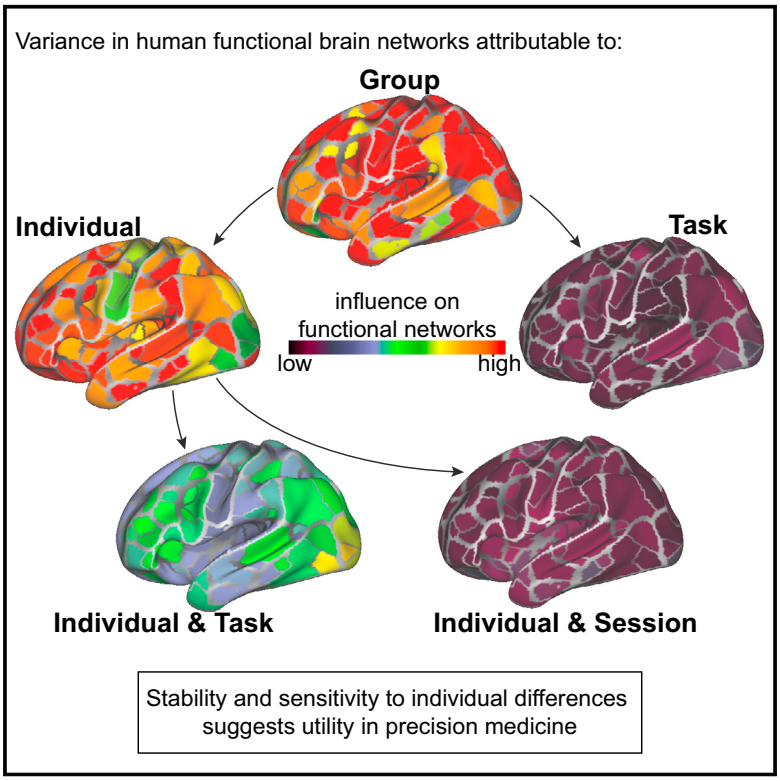

Authors

Caterina Gratton, Timothy O. Laumann, Ashley N. Nielsen, ..., Bradley L. Schlaggar, Nico U.F. Dosenbach, Steven E. Petersen

Correspondence

cgratton@wustl.edu

In Brief

Gratton et al. comprehensively measure individual, day-to-day, and task variance in functional brain networks, revealing that networks are dominated by stable individual factors, not cognitive content. These findings suggest utility of functional network measurements in personalized medicine.

Highlights

- Functional networks are dominated by common group and stable individual features
- Task state only modestly influences brain networks, largely varying by individual
- With substantial data, day-to-day variability is minimal
- Variance sources show distinct topography and links to intrinsic and evoked factors

Gratton et al., 2018, Neuron *98*, 439–452
April 18, 2018
https://doi.org/10.1016/j.neuron.2018.03.035

CellPress

Neuron
Article

Functional Brain Networks Are Dominated by Stable Group and Individual Factors, Not Cognitive or Daily Variation

Caterina Gratton,[1,12,*] Timothy O. Laumann,[2] Ashley N. Nielsen,[1] Deanna J. Greene,[2,3] Evan M. Gordon,[8,9,10] Adrian W. Gilmore,[6] Steven M. Nelson,[8,9,10,11] Rebecca S. Coalson,[1,3] Abraham Z. Snyder,[1,3] Bradley L. Schlaggar,[1,2,3,4,5] Nico U.F. Dosenbach,[1,5,7] and Steven E. Petersen[1,2,3,4,6]
[1]Department of Neurology, Washington University in St. Louis, St. Louis, MO 63110, USA
[2]Department of Psychiatry, Washington University in St. Louis, St. Louis, MO 63110, USA
[3]Department of Radiology, Washington University in St. Louis, St. Louis, MO 63110, USA
[4]Department of Neuroscience, Washington University in St. Louis, St. Louis, MO 63110, USA
[5]Department of Pediatrics, Washington University in St. Louis, St. Louis, MO 63110, USA
[6]Department of Psychological & Brain Sciences, Washington University in St. Louis, St. Louis, MO 63110, USA
[7]Program in Occupational Therapy, Washington University in St. Louis, St. Louis, MO 63110, USA
[8]VISN 17 Center of Excellence for Research on Returning War Veterans, Waco, TX 76711, USA
[9]Center for Vital Longevity, School of Behavioral and Brain Sciences, University of Texas at Dallas, Dallas, TX 75235, USA
[10]Department of Psychology and Neuroscience, Baylor University, Waco, TX 76706, USA
[11]Department of Psychiatry, Texas A&M Health Science Center, Temple, TX 76508, USA
[12]Lead Contact
*Correspondence: cgratton@wustl.edu
https://doi.org/10.1016/j.neuron.2018.03.035

SUMMARY

The organization of human brain networks can be measured by capturing correlated brain activity with fMRI. There is considerable interest in understanding how brain networks vary across individuals or neuropsychiatric populations or are altered during the performance of specific behaviors. However, the plausibility and validity of such measurements is dependent on the extent to which functional networks are stable over time or are state dependent. We analyzed data from nine high-quality, highly sampled individuals to parse the magnitude and anatomical distribution of network variability across subjects, sessions, and tasks. Critically, we find that functional networks are dominated by common organizational principles and stable individual features, with substantially more modest contributions from task-state and day-to-day variability. Sources of variation were differentially distributed across the brain and differentially linked to intrinsic and task-evoked sources. We conclude that functional networks are suited to measuring stable individual characteristics, suggesting utility in personalized medicine.

INTRODUCTION

Many long-standing questions in neuroscience, psychology, and medicine center on understanding the neural mechanisms that underlie variability in behavior, cognition, and psychopathology. A common approach to addressing these questions is to study the organization of human brain networks using fMRI, where correlations in ongoing activity can be used to capture "functional networks," groups of regions that support functions ranging from motor processing to top-down attention (Figure 1A; Biswal et al., 1995; Corbetta and Shulman, 2002; Dosenbach et al., 2007). Our ability to map functional networks in the human brain has advanced dramatically in the past decade, with precise mapping now possible both in large groups (Power et al., 2011; Yeo et al., 2011) and in individuals (Braga and Buckner, 2017; Gordon et al., 2017c; Laumann et al., 2015).

These approaches have been eagerly adopted by studies searching for insights into how brain networks reorganize with brain damage and disease (Baldassarre et al., 2016; Bassett and Bullmore, 2009; Gratton et al., 2012; Menon, 2011; Sheffield and Barch, 2016; Stam, 2014), differ across individuals (Finn et al., 2015; Gordon et al., 2017a; Gordon et al., 2017b, 2017c; Miranda-Dominguez et al., 2014; Mueller et al., 2013; Wang et al., 2015), change across the lifespan (Chan et al., 2014; Dosenbach et al., 2010; Satterthwaite et al., 2013a), and respond to different cognitive demands (Betti et al., 2013; Cole et al., 2014; Gratton et al., 2016; Krienen et al., 2014; Shine et al., 2016; Shirer et al., 2012).

In the context of these investigations, researchers often implicitly adopt one of two distinct assumptions concerning the nature of functional brain networks. One view is that functional networks mirror cognitive, perceptual, and motor processes, reconfiguring substantially with ongoing context, task demands, moods, and even fleeting thoughts. From this perspective, functional brain networks reflect dynamic activity flowing across a large set of possible network trajectories that track ongoing processing, and thus should be amenable to

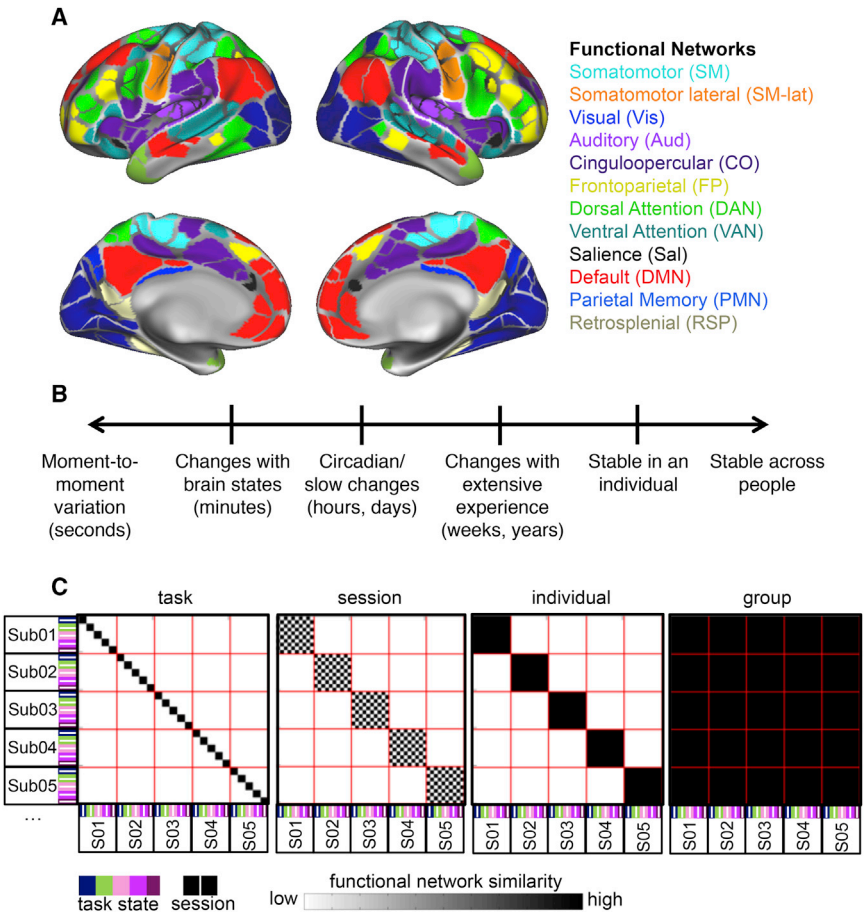

Figure 1. Scales of Variability in Functional Brain Networks

(A and B) Functional brain networks (A) may vary along different timescales (B), ranging from complete stability (with differences only attributable to sampling variability and/or measurement noise) to varying from moment-to-moment with ongoing thoughts and processes. Intermediate to these two levels, functional networks may vary on the order of minutes depending on brain state (arousal, task engagement), more slowly over the course of the day (e.g., with circadian rhythms), over the course of weeks or years (e.g., with extensive experience in a task), or they may vary across individuals.

(C) If functional brain networks are stable across people ("group," illustrated in the schematic to the right), high similarity would be expected among all measurements, even when taken from different individuals, sessions, and tasks, leading to high similarity throughout the matrix. If networks are dominated by individual variability, then high similarity would be expected of networks from the same individual (squares along the diagonal), with low similarity among networks from different individuals (middle right). Alternatively, networks that vary substantially across sessions or task states would show similarity limited to the same session (middle left) or task (left). These different sources of variability inform our understanding of the neurobiological underpinnings of functional brain networks and how they can be used to address psychological and neuropsychiatric questions concerning brain function.

See also Figure S1A.

"mind reading" applications. But, a corollary of this perspective is that functional networks would be far less useful for most clinical applications, as they would be strongly modified by the specific context under which they were measured; e.g., they could vary substantially based on the comfort of waiting rooms in a testing center or mannerisms of a technician, rather than the underlying disease. The alternative view is that functional networks are fundamentally stable, such that an fMRI scan can be used to measure network properties that are informative about a given person's stable traits (such as their disease status or personality) regardless of that person's thoughts, mood, or even behavioral task during the scan. In this view, functional networks are understood as primarily determined by structural connections that maintain a functionally stable correlation structure linked to long-term histories of co-activations between areas. If true, this would suggest that functional networks can be used for measuring individual personality traits and tracking disease, with applications in personalized medicine, but would have less utility for measuring cognitive content.

Given these opposing views, and their consequent implications for future applications of fMRI, it is important to quantify to what extent brain networks are stable or vary across time (Figure 1B). Recent work has provided evidence that functional brain networks vary across individuals, sessions, and task states (Finn et al., 2015; Geerligs et al., 2015; Gordon et al., 2017a, 2017b, 2017c; Laumann et al., 2015; Miranda-Dominguez et al., 2014; Mueller et al., 2013; Noble et al., 2017; Pannunzi et al., 2017; Xie et al., 2017). While some reports argue that brain networks are largely stable with negligible variation in networks over time during rest (Laumann et al., 2017) and subtle modifications during tasks (Cole et al., 2014; Gratton et al., 2016), other reports emphasize variability of functional networks (Allen et al., 2014; Calhoun et al., 2014; Hutchison et al., 2013) and the sensitivity of these networks to ongoing cognition (Gonzalez-Castillo et al., 2015; Shine et al., 2016; Shirer et al., 2012). These divergent accounts may arise because no study, to date, has directly contrasted the magnitude of these diverse effects. Furthermore, most previous studies have had low amounts of data per person, limiting the reliability of measurements (Laumann et al., 2015) and the ability to differentiate variability due to limitations in data quantity from individual, state, or session effects.

Here, we leverage the Midnight Scan Club (MSC) dataset (Gordon et al., 2017c), which is particularly well suited to address this question, given that it includes more than 10 hours of fMRI data from 10 highly sampled individuals across 10 different days and 5 different task states. Thus, we have sufficient data per subject, session, and task to simultaneously examine the relative contribution of (1) common (group-level) organizational principles of brain networks, (2) individually specific elements of network architecture, (3) session-dependent fluctuations in functional

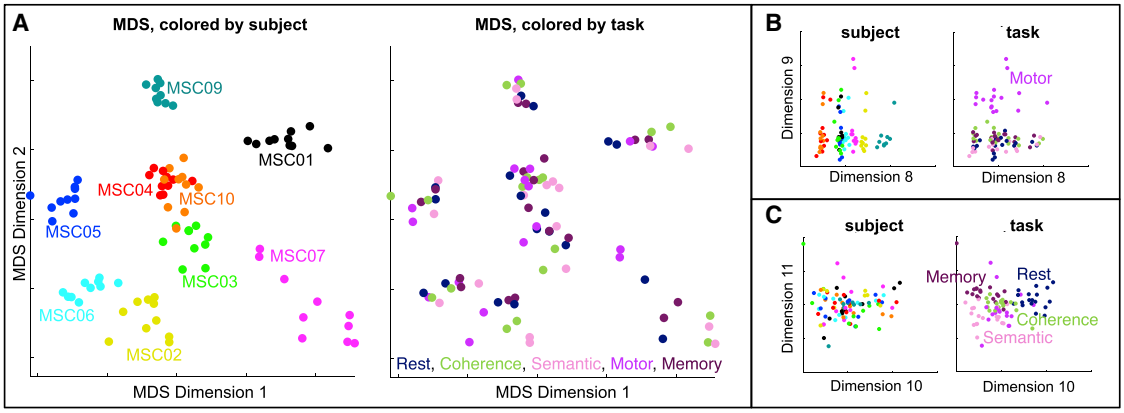

Figure 2. Multidimensional Scaling Plots of Functional Networks from Different Individuals, Tasks, and Sessions

(A–C) In these plots, each point represents a single functional network, plotted in a multidimensional space based on the similarity among networks. In the left panel, points are colored based on the participant identity of each functional network. In the right panel, points are colored based on task. (A) The first two dimensions were dominated by subject clustering, suggesting identity contributes most to functional network variance (note clustering by color in left plots). (B and C) Task-level clustering was captured at higher dimensions (note clustering by color in dimensions 8 and 9, B, and 10 and 11, C). See also Figure S1B.

networks that vary on the order of days, and (4) state-dependent variability that varies on the order of minutes during different tasks (Figure 1C). We contrast the relative magnitude of each of these effects, examine how they are distributed across the brain, and address the contribution of intrinsic and task-evoked factors.

RESULTS

Overview

The MSC dataset (Gordon et al., 2017c) includes data from ten individuals with ten separate fMRI sessions. One individual was excluded due to relatively high levels of motion (see STAR Methods). In each session, fMRI runs in five states were completed: rest (eyes open, no task) and four tasks (visual coherence, semantic, memory, and motor). Functional brain networks were measured via time-series correlations among 333 cortical regions separately for each individual, task state, and session (Figure S1A). We then examined the magnitude and anatomical distribution of group, individual, session, and task variations in these functional networks (see below). For the primary analyses reported here, we grouped data from 5 sessions into a single split-half session group to increase the total amount of data for each estimate, as large amounts of data are needed for reliable functional network estimates (Gordon et al., 2017c; Laumann et al., 2015). We also report results separated by each of the 10 sessions in the Supplemental Information.

The variability of functional networks was investigated using a combination of approaches. (1) We examined data-driven clustering of functional networks from each subject, session, and task (Figure 2). (2) We quantified the similarity of these functional networks matched on different properties (subject, session, task; Figure 3). Network similarity was used to estimate the magnitude of each "effect" (e.g., to what extent networks from the same individual are more similar than networks from different individuals). (3) We examined the anatomical distribution of each effect, both at the system (Figure 4) and region (Figure 5) levels. (4) We also examined the variance explained by each effect in single network connections (Figure 6). Finally, (5) we asked whether these effects were related to intrinsic network architecture (i.e., resting-state) or extrinsic task-evoked signals (i.e., activations during tasks; Figure 7). These analyses present convergent evidence for strong functional network stability (group and individual-dependent effects), moderate state-dependence, and minor session-dependent effects (that are likely related to data quantity). Furthermore, these effects show distinct anatomical distributions and relationships to intrinsic and extrinsic factors.

Most fMRI Network Variance Is Due to Differences across Individuals, Not Tasks or Sessions

We examined variation in functional networks in a data-driven manner using multidimensional scaling. In this approach, functional networks measured from each individual, task, and session are plotted in multidimensional space based on their similarity (Euclidean distance; similar results are obtained with correlation-based distances). As can be seen (Figure 2), most functional network clustering in the first two dimensions is driven by participant identity. Only at higher dimensions does clustering by task state appear. Session-dependent clustering was not easily discernable. Principal-component analysis demonstrates that dimensions 1–6 (dominated by subject clustering) account for a total of 48.8% of variation across functional networks (7.0%–10.1% each; see Figure S1B). Dimensions 7–12 (where clustering by task state appeared) account for a total of 19.0% of variance (1.4%–6.1% each). These findings indicate that individual variability accounts for the majority of variation between functional networks, with substantially smaller effects due to task or session.

Functional Networks Are Largely Stable with Moderate Modulations Due to Task State

We quantified similarity among functional networks for each effect directly by taking the correlation between all pairs of

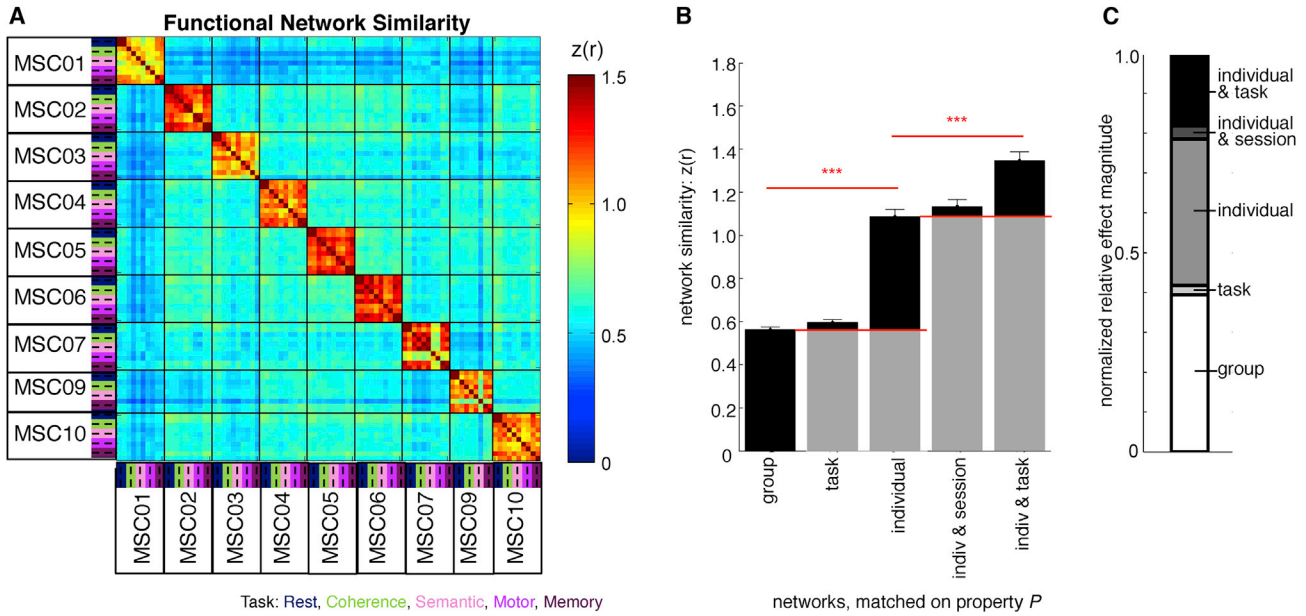

Figure 3. Quantification of the Similarity in Functional Brain Networks

(A) A similarity matrix, where every cell represents the similarity between a pair of functional networks. The matrix is organized first by individual (marked by solid black lines), then by task (colors along axes), and finally by sessions (indicated as dashed lines; here each split-half "session" represents data from 5 sessions; see Figure S2C for the similarity matrix from separated 10 sessions).

(B) Summary of similarity for networks matched on each factor, with bars of the average similarity for (1) networks across the group, from different individuals, tasks, and sessions; (2) networks from the same task but different individuals (task); (3) networks from the same individual but different sessions or task states (individual; diagonal in A); (4) networks from the same individual and session (indiv & session); or (5) networks from the same individual and task (indiv & task). The relative effects of each factor are highlighted in the black portion of each bar. Individual and task effects represent the added similarity that networks matched on either of these properties have relative to unmatched (group) networks (above the red baseline); indiv & session and indiv & task effects are the added similarity that these effects show relative to networks matched on individual identity alone (again, black portion of each bar relative to the new red baseline). Data are represented as mean ± SEM, ***p(FDR) < 0.001.

(C) To contrast the relative magnitudes of these effects, we plot the relative effect magnitudes (black portions of the bars in B), as a proportion of the total effects. Group and individual-specific effects are largest, each ~35%–40% of the total network similarity effects. Moderate individual and task interactions are also evident. Minor cross-subject task and individual and session effects were present (~5% of the total). Similar results were seen for different individuals and tasks and for matched data quantities (Figures S2A and S2B) or when non-regressed task time series are used (Figures S3A and S3B).

functional networks (i.e., the correlation of the upper triangles of correlation matrices; Figure 3).

Functional networks from different individuals, tasks, and sessions show substantial similarity (mean: z(r) = 0.56). This indicates all functional networks (the "group," background in Figure 3A) share basic structure. Networks from the same individual (i.e., squares on the diagonal in Figure 3A) were even more similar to each other, with an added effect of z(r) = 0.52 over the group effect, demonstrating a large influence of individual identity on functional networks. Thus, group and individual effects are of approximately equal magnitude.

Networks measured from the same individual and task (individual-specific task effects, mini-blocks along the diagonal within individual squares in Figure 3A) are also moderately more similar to one another than networks that are from the same individual but different tasks (an added similarity of z(r) = 0.26). This effect is approximately half as large as the individual or group effects. Cross-subject task effects (i.e., similarity among networks from the same task but different individuals) were subtle and difficult to discern but still significantly more similar than the group baseline (added similarity of z(r) = 0.04). Thus, task states modified functional networks, but these modifications largely varied by individual. Finally, networks from the same individual and session (indexing individual-specific session effects) were only slightly but significantly more similar than networks from the same individual in different sessions (added similarity of z(r) = 0.05).

All individual, session, and task effects were significantly different from their baselines (p(false discovery rate [FDR]) < 0.001). The relative magnitude of these effects was consistent across single individuals and tasks and when data quantities are matched (Figures S2A and S2B). Furthermore, similar individual, task, and session effects were seen when each session was examined separately, instead of in a split-half group (Figures S2C–S2E). Finally, similar results were obtained when complete task time series (rather than residuals after removing evoked task effects) were used in estimating task functional networks (Figures S3A and S3B). Jointly, these findings indicate that functional brain networks are dominated by stable group and individual-dependent factors, with only moderate state-based modulations. Session-dependent variation was minimal relative

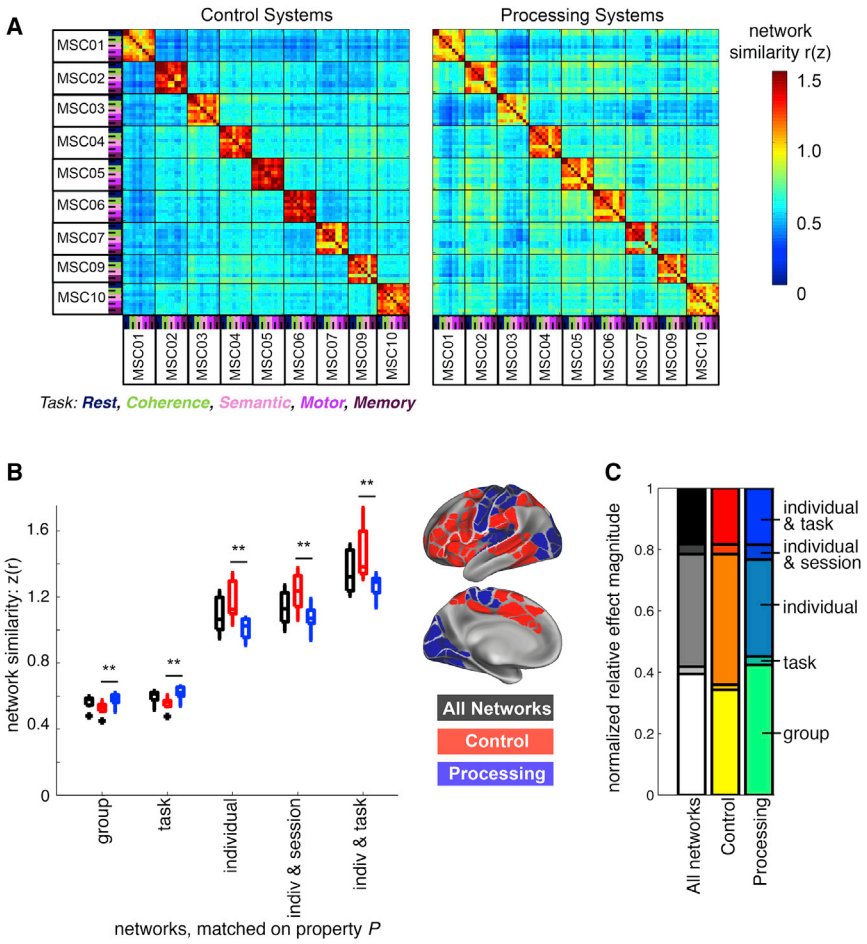

Figure 4. Individual, Task, and Session-Dependent Variation across Brain Systems

(A) Functional network similarity of top-down control (CO, FP, DAN, VAN, and Sal) and sensorimotor processing (Vis, SM, SM-lat, and Aud) systems (see anatomical distribution in bottom middle panel). Control systems show a stronger diagonal (similarity among networks from the same individual) and weaker off diagonals (similarity across subjects) relative to processing systems.

(B) Boxplots depict the average similarity for systems matched on each factor. Control systems show greater individual effects, whereas sensorimotor systems show greater cross-subject group and task effects (control versus processing, two-sided t tests, **p(FDR) < 0.01).

(C) As a comparison, we summarize the normalized relative effects for each system type (as in Figure 3C). Note again the larger individual effects in control systems, and larger group and effects in processing systems.

to the other effects, especially when data quantity per session was maximized.

Individual, Session, and Task Effects Differ by Anatomical Location

Next, we examined whether individual, task, and session effects varied by functional system and regional location.

System

First, we separately examined the magnitude of each effect for systems involved in top-down control (cinguloopercular, frontoparietal, salience, dorsal attention, and ventral attention) and sensorimotor processing (visual, auditory, somatomotor, and somatomotor lateral; Figure 4). Effects of individual identity were stronger in control than processing systems and cross-subject effects were stronger in processing than control systems (all p(FDR) < 0.01).

Region

Group, individual, task, and session effects had different spatial distributions across the brain (shown in Figure 5 as the relative normalized effect magnitude per parcel). Group factors had a large influence on parcels in the default mode and sensorimotor regions. Individual effects were most pronounced in frontoparietal and dorsal attention regions. Individual-specific task effects were strongest in a combination of control, default, and higher-level visual and motor areas, suggesting that a combination of control and processing system modulations contribute to individual-specific task modulations, despite similar overall performance on tasks across individuals.

At a different magnitude (Figure S3C), we can also see the distribution of cross-subject task effects. These were strongest in early visual and motor regions. Individual-specific session effects (Figure S3C) were strongest in areas with low fMRI signal, as well as insular and primary visual and motor regions. This pattern is suggestive of variations in fMRI signal to noise and participant drowsiness (Laumann et al., 2015). In summary, the anatomical distribution and magnitude of group, individual, session, and task-specific effects were quite different, suggesting that varied network-level mechanisms likely underlie each effect.

Variation of Single Network Edges Is Explained by Individual, Task State, and Their Interactions

To formally contrast these different sources of variation, we used a mixed-effects ANOVA to model each parcel-to-parcel functional correlation (network edge) with factors of participant identity, session, task state, and their interactions. We found that this simple model accounted for the vast majority of the variance in single connections (Figure 6; variance explained per edge, R^2 mean across edges = 0.89, SD = 0.06, max = 0.99), especially within and among control and default systems (Figure S4A).

When examined separately (Figures 6B and S4B–S4D), participant identity accounted for the majority of variance across many edges (individual ω^2, mean = 0.50, SD = 0.18, max = 0.92), especially within and between the default and control systems. Task and task-by-individual interactions accounted for a small to moderate amount of variance across a more limited distribution of edges (task ω^2, mean = 0.05, SD = 0.06, max = 0.55;

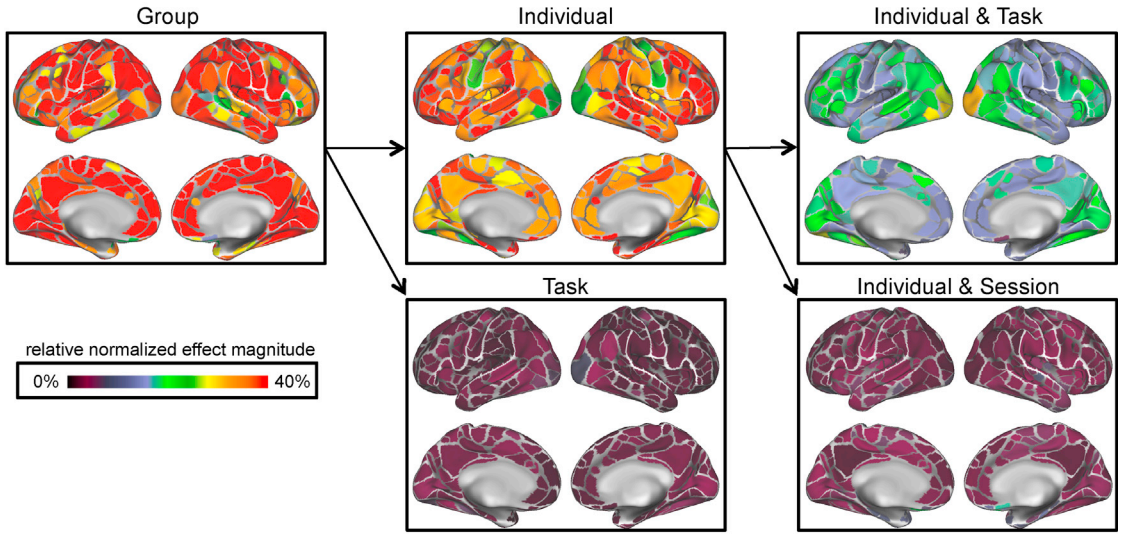

Figure 5. Individual, Task, and Session Effects across Brain Regions

The extent to which functional correlations for individual parcels are influenced by each effect (group, individual, task, individual and task, and individual and session) is examined by plotting the relative normalized effect magnitudes for each parcel (see Figure 3C). See Figure S3C for task and session effects on a narrower color scale. Individual, task, and session effects differed in distribution, suggesting the presence of differing underlying mechanisms.

task × individual ω^2, mean = 0.09, SD = 0.07, max = 0.48), primarily within and among sensorimotor and control systems. Session and session-by-individual interactions accounted for only a small portion of the variance (session ω^2, mean = 0.003, SD = 0.01, max = 0.19; session × individual ω^2, mean = 0.02, SD = 0.03, max = 0.27). The session × individual interaction was slightly higher in analyses in which the 10 sessions were analyzed separately (10-session × individual ω^2, mean = 0.05, SD = 0.04, max = 0.29; Figures S5A and S5B; note, however, the substantially lower variance explained in this version of analyses due to the increased contribution of sampling error; Figure S5A). Thus, with sufficient data, a simple model including participant identity and task state can account for most of the variability in measurements of single functional network edges.

Furthermore, we find that the addition of data-quality metrics (mean framewise displacement [FD]) for each condition does not alter the variance explained by the model (Figures S5C–S5E). This finding suggests that our rigorous preprocessing pipeline was able to address motion artifacts and that data quality does not contribute to the large individual variability present in this study.

Relationship to Intrinsic and Evoked Factors

Finally, we examined how each source of variance was related to intrinsic (resting-state architecture) and evoked (task-activations) factors.

Removal of Intrinsic Network Structure Enhances the Relative Contribution of Transient Effects

We examined how intrinsic network structure related to variation in functional networks by measuring network similarity after subtracting resting state from each task network estimate. This operation removes variability due to differences in intrinsic resting network organization (as well as parcel anatomy) between individuals and is how task-specific functional networks are often isolated (Betti et al., 2013; Cole et al., 2014; Gratton et al., 2016). Here, we ask to what extent removing intrinsic structure suppresses stable and enhances transient effects.

As expected, we find that removing resting structure strongly reduces stable effects (Figures 7A and 7B); on average, group similarity was reduced 86% (SEM = 1%) and individual similarity was reduced 73% (SEM = 4%). This indicates that a substantial portion of group and individual-specific effects were carried by intrinsic network organization and/or parcel anatomy. Intriguingly, some small group ($z(r) = 0.08$) and moderate individual similarity (added $z(r) = 0.21$ relative to group, both $p < 0.001$) remains, perhaps indexing task-general network effects. Instead, individual-specific task effects ($z(r) = 0.19$) are preserved and individual-specific session similarity ($z(r) = 0.22$) is enhanced. Thus, the relative magnitudes of these effects, especially for individual and session, are greatly increased once intrinsic structure is accounted for (compare Figure 7B, right, with Figure 3C). These findings indicate that removal of intrinsic network structure enhances the relative contribution of session and task-dependent effects in functional networks.

Interestingly, after removing rest, network similarity is higher for control than processing systems for all types of effects, including group and task (Figure S6A; $p(FDR) < 0.05$ for all effects). Thus, cross-subject effects switch from being strongest in processing systems to strongest in control systems. This finding signals the importance of accounting for intrinsic structure when studying control functions and their roles in tasks.

Evoked Signals Exhibit Low Stability and High Dependence on Task State

We also asked whether the same patterns of variability are observable in fMRI task activations. It is natural to assume that evoked signals should be strongly modulated by task state, given that task-evoked fMRI measures responses to experimental task

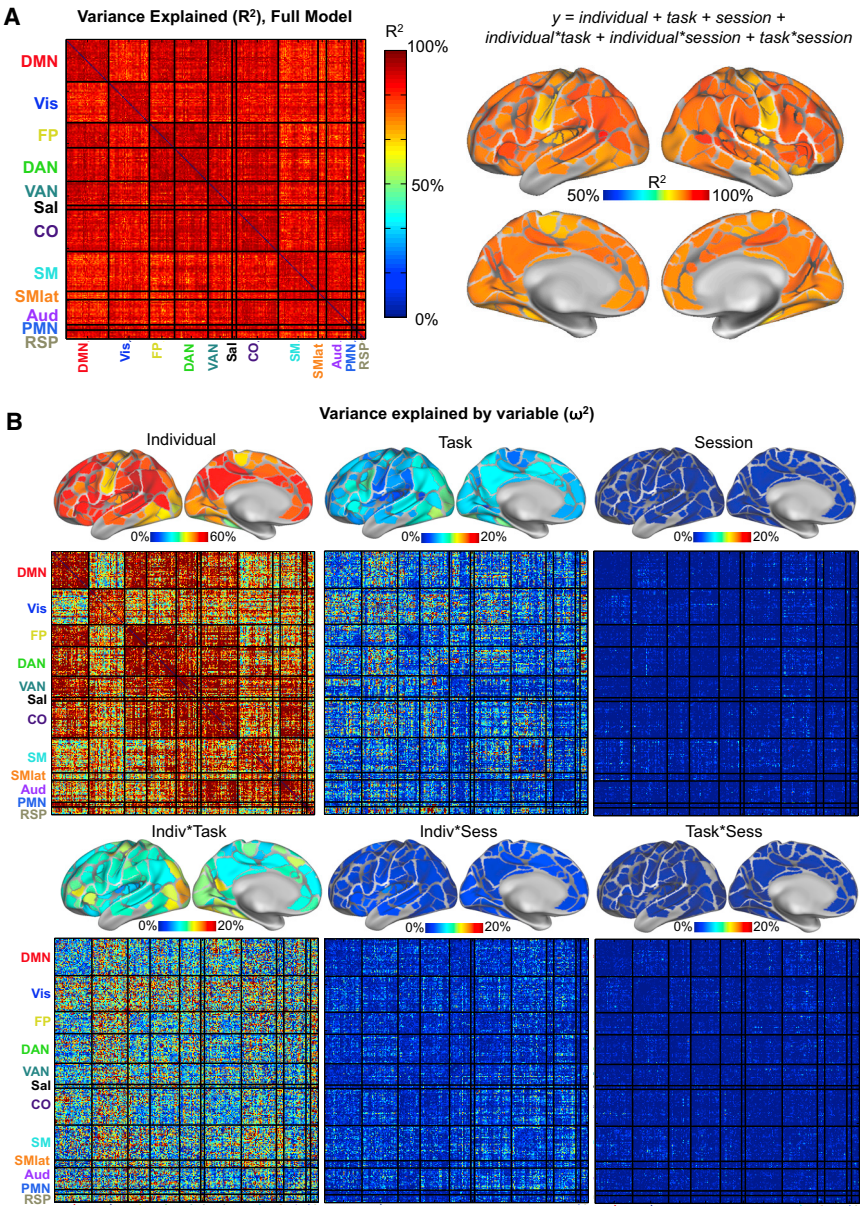

Figure 6. Modeling Variability of Single Functional Network Edges

(A) Variance in single edges was modeled with factors of individual, task state, and session, and their interactions, shown in a region-by-region correlation matrix (left). This simple model explained most of the variance in edges, with particularly high rates of variance explained within and among control and default systems (Figure S4A). Variance explained per parcel, averaged over edges (right).

(B) Variance explained (ω^2) for each factor (top, averaged over edges for a parcel; bottom, variance explained for each edge in the functional network matrix); individual identity explains the majority of the variance. Remaining variance is primarily explained by task and task X individual interactions (particularly in higher-level processing and control regions). Session related variance was minor, but slightly higher in the analysis conducted on 10 separated sessions rather than split-half (Figures S5A and S5B).

manipulations. However, many findings suggest that task-evoked (first order) signals are intimately related to (second order) functional connectivity measurements, with observations that networks formed from co-activations during tasks strongly resemble functional networks from spontaneous firing at rest (Smith et al., 2009). This relationship is proposed to stem from (1) evoked signals shaping intrinsic network structure historically, as repeated co-activations may mediate stronger Hebbian-like connections between regions and thereby stronger spontaneous correlations (Dosenbach et al., 2007), and/or (2) evoked signals directly contributing to functional network measurements, as activations "flow" through a network, influencing correlation structure (Cole et al., 2016). Thus, this logic suggests that task-evoked signals may be strongly related to functional networks and will show related patterns of variability.

To address this question, we conducted the same form of analyses for activations from each individual, task, and session (see STAR Methods; for task activations, we examined percent signal change across all conditions and again grouped sessions into split halves to increase data quantity). Interestingly, the variability profile of activation maps is very different from the similarity among functional networks (Figures 7B and 7C). There is lower similarity among activation maps across individuals (diagonal), and much of this is dominated by similarity in activations among the same task from a given individual (mini-squares along the diagonal). Instead, there is stronger similarity in activations from the same task across individuals (note vertical/horizontal lines; the motor task stands out as most distinct task). See Figures S6D–S6F for extended analyses and modeling by parcel.

These findings indicate that evoked signals have a distinct profile of variance along the state-to-stable continuum. Evoked signals likely contribute little to stable individual-dependent variability but more strongly to task and individual-specific task variability. Jointly, these results indicate that functional network measures are better suited for individual-level identification than tracking ongoing cognitive processes, which are better quantified via evoked measurements.

DISCUSSION

In this study, we asked how functional brain networks vary over different timescales. We examined the magnitude and

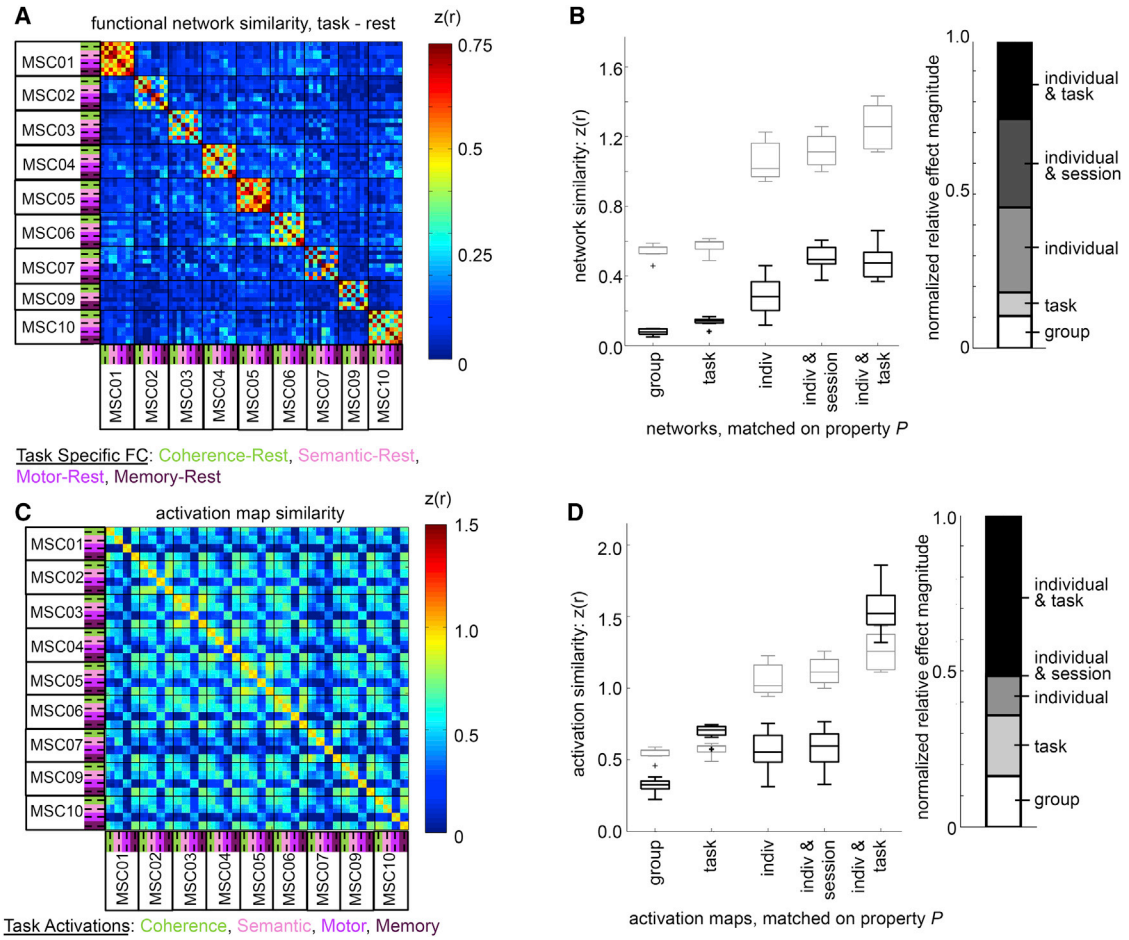

Figure 7. Relationship of Variability to Intrinsic and Task-Evoked Factors

(A) The similarity among functional networks during tasks is depicted, after subtracting resting intrinsic structure from each functional network matrix. Notably, similarity values are reduced, but block structure (i.e., individual-specific effects) remains along the diagonal. Mini-blocks along the diagonal (indicating individual-specific task effects), and off-diagonal lines (indicating session effects) are now more clearly evident.

(B) The similarity for networks matched on different factors (black boxplots). As suggested in (A), network similarity was strongly reduced relative to the original networks (light gray boxplots, Figure 3; for comparison, light-gray bars were calculated without the rest condition). However, individual and session, individual and task, and cross-subject task effects remain and are enhanced in relative magnitude (right). See Figures S6A–S6C for additional comparisons of functional networks after subtracting rest.

(C) Similarity of task activation maps across individuals, sessions, and tasks. Note that unlike in (A) and Figure 3, there is reduced block structure along the diagonal, primarily dominated by mini-blocks indicating a high similarity of task-specific activation maps within an individual. The motor task is most different from others in its activation pattern.

(D) Quantification of the similarity of activation maps across different factors (black). Unlike the similarity of the original functional networks (light gray, again without rest for comparison), task- and individual and task effects are larger, with only moderate individual and group effects. See Figures S6D–S6F for additional comparisons and modeling analyses.

anatomical distribution of individual, session, and state variability in the Midnight Scan Club dataset, which contains substantial amounts of data for nine high-quality subjects, from 10 days, in five states, allowing us to simultaneously contrast the influence of these factors. We find that functional networks are primarily stable, with moderate state-based modulations that varied largely across individuals. With large amounts of data, session-dependent variability was minor. These forms of variance were distributed differently across the brain, with individual variability strongest in control systems and state- and session-dependent variability stronger in processing systems. Finally, intrinsic resting structure and evoked signal variability were linked to stable and state-dependent variability, respectively. These observations have consequences for research and medical applications of brain network mapping, as they indicate that (1) functional networks are best suited to measuring stable characteristics of individuals; (2) an individual's state also moderately influences network organization, suggesting that state-changes should be accounted for in network comparisons; and (3) session-dependent variation can be minimized with large amounts of data.

Functional Brain Networks Are Largely Stable

Our findings suggest robust contributions from both common organizational principles and stable variation between individuals to functional brain networks. These findings indicate that the majority of functional network organization arises from stable factors, such as genetics, structural connections, and long-term histories of co-activation among regions, rather than more transient factors, such as ongoing cognition or day-to-day fluctuations.

The large subject-level effects in functional networks highlights the importance of individualized approaches for studying properties of brain organization. Large amounts of high-quality data are needed to enable precise measurement of functional networks (Braga and Buckner, 2017; Gordon et al., 2017c; Laumann et al., 2015) and tease apart true network differences from sampling variability, motion, or other artifacts (Laumann et al., 2017; Power et al., 2012). Individual-specific effects on functional networks (also reported by Finn et al., 2015; Gordon et al., 2017a, 2017b, 2017c; Laumann et al., 2015; Miranda-Dominguez et al., 2014; Mueller et al., 2013) are likely driven by a combination of functional and anatomical variability. The anatomical location of brain areas may be shifted, expanded, or contracted across individuals (Gordon et al., 2017b), leading to consistent alterations in network estimates, or variation may exist in the functional correlation magnitudes themselves. While it is difficult to tease apart structural and functional contributions to individual variability, previous work suggests that gross anatomical misalignment does not contribute to the majority of individual differences in functional networks (Gordon et al., 2017b). Furthermore, examining the similarity of networks composed of individually optimized, rather than group, parcels (matched at the network level) only slightly diminishes individual effects in favor of group similarity (Figure S7). This observation suggests that individual effects do not arise entirely from differences in the anatomical distribution of networks across individuals but may reflect differences across individuals in the magnitude of connectivity within and between networks. Future work adopting hyper-alignment (Guntupalli et al., 2016; Guntupalli and Haxby, 2017) or related techniques may help to clarify the contribution of individual differences in spatial mapping from differences in connectivity magnitude.

What is additionally clear from this report is that a great deal of functional network architecture is consistent across individuals; indeed, functional networks can largely be described as variations on a central theme. This robust group effect may underlie the success of past group approaches in the study of functional brain networks (Power et al., 2011; Yeo et al., 2011). However, our findings also suggest that a group description, alone, will fall short of describing functional brain networks at a level of precision that may be most impactful clinically.

Furthermore, group and individual effects were localized differently; group effects were strongest in processing (e.g., sensorimotor) regions whereas individual effects were most prominent in control, especially frontoparietal regions, consistent with past reports (Finn et al., 2015; Gordon et al., 2017b; Miranda-Dominguez et al., 2014; Mueller et al., 2013). This suggests that individual-specific measurements may be especially important in applications targeting these high-level systems and their functions. The default mode (DMN), in this experiment, appears intermediate to control and processing systems; it exhibits high group similarity but intermediate individual-level effects. These findings and other numerous results linking the DMN to de-activations during most tasks, unlike either control or processing systems (Raichle et al., 2001; Shulman et al., 1997), but with activations proportional to task load like control systems (McKiernan et al., 2003; Singh and Fawcett, 2008) and with peripheral position in network graphs like processing systems (Gratton et al., 2016; Power et al., 2013), suggest that the DMN does not neatly fall into either control or processing categories.

Task States Moderately Modify Networks, and Modulations Are Largely Individual-Specific

Although functional brain networks are primarily characterized by stability, we also found evidence that task states modify brain networks. Intriguingly, the majority of task modulations varied by individual; common task modulations (i.e., task-specific network changes consistent across subjects) were subtle, but individual-specific task effects were about half of the size of individual variability alone, a moderate influence on functional network measurements.

These findings provide context to previous reports of subtle differences in functional networks seen in different tasks across subjects (Cole et al., 2014; Gratton et al., 2016; Krienen et al., 2014). Task states clearly influence functional networks, but our results demonstrate that cross-subject modulations are relatively small (~5%). Thus, detection of common task effects will likely require large amounts of high-quality data (e.g., >20 min, as in Gratton et al., 2016), along with targeted removal of the substantially larger stable effects (e.g., by removing intrinsic structure; Figure 7; Betti et al., 2013; Cole et al., 2014; Gratton et al., 2016; see also Xie et al., 2017).

The larger individual-specific task effects on brain networks (~5% cross-subject versus ~20% individual specific) emphasize that individual-specific analyses may be a more productive avenue for investigating task-based modulations of brain networks. These findings expand upon previous studies (Geerligs et al., 2015; Xie et al., 2017), which have suggested that task and individual variability interact. Notably, we found large individual differences in task effects even though many of the tasks were fairly simple (e.g., move a hand, categorize faces as male or female, identify if dots are arranged concentrically) with high levels of performance across all participants. These individual by task interactions remained present after the removal of intrinsic network structure, indicating that they do not arise linearly from intrinsic functional/anatomical differences between regions. One possibility is that they index the presence of multiple neural or cognitive strategies for completing even simple tasks (e.g., how hard to squeeze a hand; Fox et al., 2007; Pearce and Moran, 2012). While the magnitude of task by individual interactions differed by task, as predicted by Finn et al. (2017), inter-task differences were minor compared to the overall size of the individual-specific task effect and at least partly dependent on data quantity/quality (Figure S2); future work will be needed to determine the importance of these differences.

With Sufficient Data, Functional Networks Exhibit Low Variability across Days

Recent work has brought attention to the contribution of day-to-day variability in functional brain networks (Noble et al., 2017; Pannunzi et al., 2017). We also find significant session variability, yet these effects were small relative to group, individual, or task differences, whether examined in split-half sessions or by 10-session groupings. The small session-dependent variability is at least partly attributable to the large quantity of data present in this study, which decreases the extent of variability due to sampling error (Laumann et al., 2015). Importantly, unlike previous studies (Gordon et al., 2017c; Laumann et al., 2015) that examined session effects by looking at variance across runs in different sessions, we examined session effects that were consistent across all scans within a given session, such that random sampling noise would be less likely to contribute to our estimates. Therefore, our estimates of session variability may be lower than others that do not separate consistent session variability from random noise. Finally, scan times were precisely controlled in the present study (12–2 a.m.), decreasing variability due to circadian factors. Thus, session-dependent effects are likely minor contributors to variability in precisely phenotyped data (Gordon et al., 2017c) but may have larger contributions in datasets with shorter quantities of data per session or more variable times of acquisition.

Of note, session variability was consistently smaller than variability across tasks in individuals, and these two forms of variability had different anatomical distributions. The topography of session variability (in low-signal regions as well as motor, visual, and cinguloopercular systems) resembles previous reports (Gordon et al., 2017c; Laumann et al., 2015) and at least partly overlaps with effects of drowsiness (Laumann et al., 2017; Mitra et al., 2015; Tagliazucchi and Laufs, 2014), suggesting that individual differences in drowsiness across sessions may contribute. Furthermore, session-dependent variability could also be attributable to variability in data acquisition, fMRI signal, or other systematic biases on data quality.

The Majority of Variability of Single Functional Connections Is Related to Individual and Task

Our study demonstrates that a simple model, with factors of individual, task, session, and their interactions, accounts for the vast majority of the variance in functional networks, even in single functional connections—averaging at 89% of variance explained. This finding is exciting, as it predicts that given sufficient data, we may be able to robustly measure single network edges, and estimate their likely contribution from more temporary (i.e., task state) and stable (i.e., individual) factors. This may be a fruitful avenue to pursue in medical applications of the technique. Consistent with other findings here, variance in single functional connections was largely attributable to individual variability, with moderate contributions of task state.

Evoked Signals Are Less Reflective of Stable Brain Features than Functional Connectivity

In contrast to the high stability of functional networks, task activations show diminished stability (i.e., across individuals and the group) and increased task dependence. These findings indicate distinct patterns of variation in first- (activation) and second-order (correlation) fMRI signals. At first blush, this may not be surprising, given that activation signals measure task-locked effects. However, one might have predicted that individual differences in network architecture would map onto individual differences in task activations (e.g., as shown in Gordon et al., 2017c; Smith et al., 2009; Tavor et al., 2016), and, thereby, task activations would also exhibit robust individual differences similar to functional networks. Our findings suggest that these two measures, while related, may not correspond simply (Gratton et al., 2016).

One possibility is that evoked signals show higher task effects than functional connectivity because they are compared with a baseline condition. However, subtracting the intrinsic resting baseline from task functional networks to isolate task-specific signals does not augment transient task effects in functional networks to the level seen in activations (compare Figure 7D to Figure 7B).

Removal of Intrinsic Signals Emphasizes Transient Effects

Studies investigating how functional networks respond to transient events, such as tasks or ongoing cognition, often attempt to isolate these features by subtracting intrinsic resting-state structure from task networks to produce task-specific network measurements (Cole et al., 2014; Gratton et al., 2016). We examined how this operation affected variability in functional networks. Subtraction of intrinsic network architecture decreased group and individual effects (85% and 69%, respectively) while relatively preserving or enhancing state- and session-dependent variability. Thus, consistent with past endeavors, intrinsic signal removal may help to uncover more transient functional network signals. However, as noted above, this operation still falls short of producing task effects of the magnitude seen with evoked measures. Furthermore, neither group nor individual-specific similarity was fully removed with rest subtraction, suggesting the presence of nonspecific task-general states (i.e., effects that are commonly found within/across individuals in all tasks, but not rest, and thus remain after rest subtraction; Cole et al., 2014; Gratton et al., 2016).

Spanning from States to Stability in Functional Brain Networks

As detailed above, this study contrasts the effects of session, task, and individual variability on functional brain networks. Previous work from our lab (Laumann et al., 2017) has also examined more transient functional network "dynamics" (i.e., time-varying changes in functional networks) within a scan, finding little evidence for time-varying changes in functional networks at rest, once artifacts and state changes (drowsiness, task) are accounted for (see also Hindriks et al., 2016; Liégeois et al., 2017). Jointly, our findings indicate that functional brain networks, as measured with slow fluctuations of the blood-oxygen-level-dependent (BOLD) signal, are strongly weighted toward stable information and provide less information about more transient aspects of neural processing.

It is worth noting that our study does not cover the full state-to-stable spectrum. Sessions in this study were completed within a

few weeks and do not provide estimates of the stability of functional networks at longer timescales. High stability has been demonstrated in functional networks over the course of a year (Poldrack et al., 2015), but networks have also been shown to vary meaningfully over the lifespan (Chan et al., 2014; Greene et al., 2014; Satterthwaite et al., 2013a), allowing for the robust decoding of participant age (Dosenbach et al., 2010; Fair et al., 2013; Satterthwaite et al., 2013b). We also do not examine how functional networks change with extended training or experience. Previous findings (Bassett et al., 2011; Lewis et al., 2009) suggest training has measurable, but subtle, influences. Future work will be needed to directly contrast lifespan and experience-based changes with the effects measured here.

Finally, we note that this manuscript is exclusively focused on low-frequency functional brain networks, as measured with time-series correlations of the BOLD signal in fMRI. These findings are highly pertinent to the neuroscientific community, given the widespread use of fMRI network-based approaches to address both clinical and psychological questions. However, signals at higher frequencies (e.g., as might be measured with electroencephalogram [EEG] or magnetoencephalography [MEG]) or techniques focused on alternative aspects of BOLD network interactions (e.g., lag; Mitra and Raichle, 2016) may be more amenable to tracking state-dependent variability.

Implications for Scientific and Medical Applications of Functional Networks

The current work has clear implications for both scientific and medical applications of functional network mapping. Scientifically, these findings indicate that studies of functional network differences between populations and task conditions are likely to be dominated by stable factors with moderate state-based effects and that care must be taken to isolate the desired component. Thus, successful past studies measuring differences in brain networks with disease (see Baldassarre et al., 2016; Bassett and Bullmore, 2009; Greene et al., 2016; Menon, 2011; Sheffield and Barch, 2016; Stam, 2014) are most likely underpinned by differences in a stable network architecture, although comparisons are best made if studies also avoid contamination from state-based differences such as might occur with different levels of sleep between groups (Tagliazucchi and Laufs, 2014) or, in task or movie paradigms, with differing engagement in the presented material (Greene et al., 2018). Given the relatively small magnitude of most published effects of disease on brain networks, both sources of variance may meaningfully affect interpretations.

Our findings also emphasize the large size of individual-specific effects. Neglect of individual differences in brain networks may cause researchers to miss substantial and relevant portions of variability in the data. Importantly, this conclusion also applies to studies of how tasks modify brain networks; the bulk of task-based effects in this study were individually specific, suggesting that without individual-level analysis, these large effects may be obscured. However, as previously demonstrated (Gordon et al., 2017c; Laumann et al., 2015), large quantities of artifact-free data are needed to accurately measure brain networks in the face of sampling variability. Jointly, our findings prescribe a move toward longer and/or multiple resting-state scans per individual.

Clinically, the highly stable nature of functional networks is extremely promising for medical applications, suggesting that they may be good candidates for biomarkers and surgical planning (Kamran et al., 2014). However, as noted above, these findings indicate that clinical uses of functional networks will be most accurate if they are optimized separately for each individual, consistent with the trend for higher-quality personalized medicine approaches. Furthermore, the moderate size of task-based effects suggests that measuring brain networks across different states (e.g., as is done in clinical EEG) may help maximize diagnostic value (Finn et al., 2017), especially for certain regions of the brain, including higher-level control networks. Indeed, one might imagine that the risks of brain surgery would warrant careful delineation of networks across many different contexts.

Conclusion

Here, we asked to what extent functional brain networks vary over different timescales. We find that functional brain networks measured with fMRI are largely stable, dominated by contributions from common organizational principles and stable individual features. Functional networks also vary moderately across task states, largely in an individual-specific manner. With sufficient data, we found that session-dependent variability was minor. These findings have important implications for functional network mapping, suggesting that the technique is well suited to measuring stable individual differences associated with personality traits or disease and may hold promise for identifying biomarkers. Furthermore, they emphasize the utility of a precision individual approach in the delineation of functional network architecture.

STAR★METHODS

Detailed methods are provided in the online version of this paper and include the following:

- KEY RESOURCES TABLE
- CONTACT FOR REAGENT AND RESOURCE SHARING
- EXPERIMENTAL MODEL AND SUBJECT DETAILS
  - Participants and Study Design
- METHOD DETAILS
  - MRI Data Acquisition
  - Task Designs and Analysis
- QUANTIFICATION AND STATISTICAL ANALYSES
  - MRI Data Processing and Surface Registration
  - Functional Networks
  - Analysis Overview
- DATA AND SOFTWARE AVAILABILITY

SUPPLEMENTAL INFORMATION

Supplemental Information includes seven figures and can be found with this article online at https://doi.org/10.1016/j.neuron.2018.03.035.

ACKNOWLEDGMENTS

This work is supported by NIH grants F32NS092290 (C.G.), NS088590 and TR000448 (N.U.F.D.), MH100872 (T.O.L.), MH104592 (D.J.G.), 1P30NS098577 (Neuroimaging Informatics and Analysis Center), and HD087011 (Intellectual

and Developmental Disabilities Research Center at Washington University); Jacobs Foundation grant 2016121703 (N.U.F.D.); the Child Neurology Foundation (N.U.F.D); the McDonnell Center for Systems Neuroscience (N.U.F.D. and B.L.S.); Mallinckrodt Institute of Radiology grant 14-011 (N.U.F.D.); the Hope Center for Neurological Disorders (N.U.F.D., B.L.S., S.E.P.); an American Psychological Association dissertation research award (A.W.G.); and Dart Neuroscience LLC. The views expressed in this article are those of the authors and do not necessarily reflect the position or policy of the Department of Veterans Affairs or the U.S. government.

AUTHOR CONTRIBUTIONS

Conceptualization, C.G. and S.E.P.; Methodology, Software and Formal Analysis, C.G., T.O.L., A.N.N., D.J.G., E.M.G., A.W.G., S.M.N., R.S.C., A.Z.S, B.L.S., N.U.F.D., and S.E.P.; Data Curation, T.O.L., A.W.G., R.S.C., and N.U.F.D.; Writing, C.G., T.O.L., A.N.N., D.J.G., E.M.G., A.W.G., S.M.N., R.S.C., A.Z.S, B.L.S., N.U.F.D., and S.E.P.; Supervision, S.E.P., N.U.F.D., and B.L.S.; Funding Acquisition, C.G., S.E.P., N.U.F.D., and B.L.S.

DECLARATION OF INTERESTS

The authors declare no competing interests.

Received: November 19, 2017
Revised: February 20, 2018
Accepted: March 20, 2018
Published: April 18, 2018

REFERENCES

Al-Aidroos, N., Said, C.P., and Turk-Browne, N.B. (2012). Top-down attention switches coupling between low-level and high-level areas of human visual cortex. Proc. Natl. Acad. Sci. USA *109*, 14675–14680.

Allen, E.A., Damaraju, E., Plis, S.M., Erhardt, E.B., Eichele, T., and Calhoun, V.D. (2014). Tracking whole-brain connectivity dynamics in the resting state. Cereb. Cortex *24*, 663–676.

Baldassarre, A., Ramsey, L.E., Siegel, J.S., Shulman, G.L., and Corbetta, M. (2016). Brain connectivity and neurological disorders after stroke. Curr. Opin. Neurol. *29*, 706–713.

Balota, D.A., Yap, M.J., Cortese, M.J., Hutchison, K.A., Kessler, B., Loftis, B., Neely, J.H., Nelson, D.L., Simpson, G.B., and Treiman, R. (2007). The English Lexicon Project. Behav. Res. Methods *39*, 445–459.

Barch, D.M., Burgess, G.C., Harms, M.P., Petersen, S.E., Schlaggar, B.L., Corbetta, M., Glasser, M.F., Curtiss, S., Dixit, S., Feldt, C., et al.; WU-Minn HCP Consortium (2013). Function in the human connectome: task-fMRI and individual differences in behavior. Neuroimage *80*, 169–189.

Bassett, D.S., and Bullmore, E.T. (2009). Human brain networks in health and disease. Curr. Opin. Neurol. *22*, 340–347.

Bassett, D.S., Wymbs, N.F., Porter, M.A., Mucha, P.J., Carlson, J.M., and Grafton, S.T. (2011). Dynamic reconfiguration of human brain networks during learning. Proc. Natl. Acad. Sci. USA *108*, 7641–7646.

Betti, V., Della Penna, S., de Pasquale, F., Mantini, D., Marzetti, L., Romani, G.L., and Corbetta, M. (2013). Natural scenes viewing alters the dynamics of functional connectivity in the human brain. Neuron *79*, 782–797.

Biswal, B., Yetkin, F.Z., Haughton, V.M., and Hyde, J.S. (1995). Functional connectivity in the motor cortex of resting human brain using echo-planar MRI. Magn. Reson. Med. *34*, 537–541.

Braga, R.M., and Buckner, R.L. (2017). Parallel interdigitated distributed networks within the individual estimated by intrinsic functional connectivity. Neuron *95*, 457–471.

Calhoun, V.D., Miller, R., Pearlson, G., and Adalı, T. (2014). The chronnectome: time-varying connectivity networks as the next frontier in fMRI data discovery. Neuron *84*, 262–274.

Chan, M.Y., Park, D.C., Savalia, N.K., Petersen, S.E., and Wig, G.S. (2014). Decreased segregation of brain systems across the healthy adult lifespan. Proc. Natl. Acad. Sci. USA *111*, E4997–E5006.

Cohen, J. (1973). Eta-squared and partial eta-squared in fixed factor ANOVA designs. Educ. Psychol. Meas. *33*, 107–112.

Cole, M.W., Bassett, D.S., Power, J.D., Braver, T.S., and Petersen, S.E. (2014). Intrinsic and task-evoked network architectures of the human brain. Neuron *83*, 238–251.

Cole, M.W., Ito, T., Bassett, D.S., and Schultz, D.H. (2016). Activity flow over resting-state networks shapes cognitive task activations. Nat. Neurosci. *19*, 1718–1726.

Corbetta, M., and Shulman, G.L. (2002). Control of goal-directed and stimulus-driven attention in the brain. Nat. Rev. Neurosci. *3*, 201–215.

Dale, A.M., Fischl, B., and Sereno, M.I. (1999). Cortical surface-based analysis. I. Segmentation and surface reconstruction. Neuroimage *9*, 179–194.

Dosenbach, N.U., Fair, D.A., Miezin, F.M., Cohen, A.L., Wenger, K.K., Dosenbach, R.A., Fox, M.D., Snyder, A.Z., Vincent, J.L., Raichle, M.E., et al. (2007). Distinct brain networks for adaptive and stable task control in humans. Proc. Natl. Acad. Sci. USA *104*, 11073–11078.

Dosenbach, N.U., Nardos, B., Cohen, A.L., Fair, D.A., Power, J.D., Church, J.A., Nelson, S.M., Wig, G.S., Vogel, A.C., Lessov-Schlaggar, C.N., et al. (2010). Prediction of individual brain maturity using fMRI. Science *329*, 1358–1361.

Dubis, J.W., Siegel, J.S., Neta, M., Visscher, K.M., and Petersen, S.E. (2016). Tasks driven by perceptual information do not recruit sustained BOLD activity in cingulo-opercular regions. Cereb. Cortex *26*, 192–201.

Fair, D.A., Schlaggar, B.L., Cohen, A.L., Miezin, F.M., Dosenbach, N.U., Wenger, K.K., Fox, M.D., Snyder, A.Z., Raichle, M.E., and Petersen, S.E. (2007). A method for using blocked and event-related fMRI data to study "resting state" functional connectivity. Neuroimage *35*, 396–405.

Fair, D.A., Nigg, J.T., Iyer, S., Bathula, D., Mills, K.L., Dosenbach, N.U., Schlaggar, B.L., Mennes, M., Gutman, D., Bangaru, S., et al. (2013). Distinct neural signatures detected for ADHD subtypes after controlling for micro-movements in resting state functional connectivity MRI data. Front. Syst. Neurosci. *6*, 80.

Finn, E.S., Shen, X., Scheinost, D., Rosenberg, M.D., Huang, J., Chun, M.M., Papademetris, X., and Constable, R.T. (2015). Functional connectome fingerprinting: identifying individuals using patterns of brain connectivity. Nat. Neurosci. *18*, 1664–1671.

Finn, E.S., Scheinost, D., Finn, D.M., Shen, X., Papademetris, X., and Constable, R.T. (2017). Can brain state be manipulated to emphasize individual differences in functional connectivity? Neuroimage *160*, 140–151.

Fox, M.D., Snyder, A.Z., Vincent, J.L., and Raichle, M.E. (2007). Intrinsic fluctuations within cortical systems account for intertrial variability in human behavior. Neuron *56*, 171–184.

Geerligs, L., Rubinov, M., Cam-Can, and Henson, R.N. (2015). State and trait components of functional connectivity: individual differences vary with mental state. J. Neurosci. *35*, 13949–13961.

Glass, L. (1969). Moiré effect from random dots. Nature *223*, 578–580.

Glasser, M.F., Sotiropoulos, S.N., Wilson, J.A., Coalson, T.S., Fischl, B., Andersson, J.L., Xu, J., Jbabdi, S., Webster, M., Polimeni, J.R., et al.; WU-Minn HCP Consortium (2013). The minimal preprocessing pipelines for the Human Connectome Project. Neuroimage *80*, 105–124.

Gonzalez-Castillo, J., Hoy, C.W., Handwerker, D.A., Robinson, M.E., Buchanan, L.C., Saad, Z.S., and Bandettini, P.A. (2015). Tracking ongoing cognition in individuals using brief, whole-brain functional connectivity patterns. Proc. Natl. Acad. Sci. USA *112*, 8762–8767.

Gordon, E.M., Laumann, T.O., Adeyemo, B., Huckins, J.F., Kelley, W.M., and Petersen, S.E. (2016). Generation and evaluation of a cortical area parcellation from resting-state correlations. Cereb. Cortex *26*, 288–303.

Gordon, E.M., Laumann, T.O., Adeyemo, B., Gilmore, A.W., Nelson, S.M., Dosenbach, N.U.F., and Petersen, S.E. (2017a). Individual-specific features

of brain systems identified with resting state functional correlations. Neuroimage *146*, 918–939.

Gordon, E.M., Laumann, T.O., Adeyemo, B., and Petersen, S.E. (2017b). Individual variability of the system-level organization of the human brain. Cereb. Cortex *27*, 386–399.

Gordon, E.M., Laumann, T.O., Gilmore, A.W., Newbold, D.J., Greene, D.J., Berg, J.J., Ortega, M., Hoyt-Drazen, C., Gratton, C., Sun, H., et al. (2017c). Precision functional mapping of individual human brains. Neuron *95*, 791–807.

Gratton, C., Nomura, E.M., Pérez, F., and D'Esposito, M. (2012). Focal brain lesions to critical locations cause widespread disruption of the modular organization of the brain. J. Cogn. Neurosci. *24*, 1275–1285.

Gratton, C., Laumann, T.O., Gordon, E.M., Adeyemo, B., and Petersen, S.E. (2016). Evidence for two independent factors that modify brain networks to meet task goals. Cell Rep. *17*, 1276–1288.

Greene, D.J., Laumann, T.O., Dubis, J.W., Ihnen, S.K., Neta, M., Power, J.D., Pruett, J.R., Jr., Black, K.J., and Schlaggar, B.L. (2014). Developmental changes in the organization of functional connections between the basal ganglia and cerebral cortex. J. Neurosci. *34*, 5842–5854.

Greene, D.J., Church, J.A., Dosenbach, N.U., Nielsen, A.N., Adeyemo, B., Nardos, B., Petersen, S.E., Black, K.J., and Schlaggar, B.L. (2016). Multivariate pattern classification of pediatric Tourette syndrome using functional connectivity MRI. Dev. Sci. *19*, 581–598.

Greene, D.J., Koller, J.M., Hampton, J.M., Wesevich, V., Van, A.N., Nguyen, A.L., Hoyt, C.R., McIntyre, L., Earl, E.A., Klein, R.L., et al. (2018). Behavioral interventions for reducing head motion during MRI scans in children. Neuroimage *171*, 234–245.

Guntupalli, J.S., and Haxby, J.V. (2017). A computational model of shared fine-scale structure in the human connectome. bioRxiv. https://doi.org/10.1101/108738.

Guntupalli, J.S., Hanke, M., Halchenko, Y.O., Connolly, A.C., Ramadge, P.J., and Haxby, J.V. (2016). A model of representational spaces in human cortex. Cereb. Cortex *26*, 2919–2934.

Hindriks, R., Adhikari, M.H., Murayama, Y., Ganzetti, M., Mantini, D., Logothetis, N.K., and Deco, G. (2016). Can sliding-window correlations reveal dynamic functional connectivity in resting-state fMRI? Neuroimage *127*, 242–256.

Hutchison, R.M., Womelsdorf, T., Allen, E.A., Bandettini, P.A., Calhoun, V.D., Corbetta, M., Della Penna, S., Duyn, J.H., Glover, G.H., Gonzalez-Castillo, J., et al. (2013). Dynamic functional connectivity: promise, issues, and interpretations. Neuroimage *80*, 360–378.

Kamran, M., Hacker, C.D., Allen, M.G., Mitchell, T.J., Leuthardt, E.C., Snyder, A.Z., and Shimony, J.S. (2014). Resting-state blood oxygen level-dependent functional magnetic resonance imaging for presurgical planning. Neuroimaging Clin. N. Am. *24*, 655–669.

Krienen, F.M., Yeo, B.T., and Buckner, R.L. (2014). Reconfigurable task-dependent functional coupling modes cluster around a core functional architecture. Philos. Trans. R. Soc. Lond. B Biol. Sci. *369*, 20130526.

Laumann, T.O., Gordon, E.M., Adeyemo, B., Snyder, A.Z., Joo, S.J., Chen, M.Y., Gilmore, A.W., McDermott, K.B., Nelson, S.M., Dosenbach, N.U., et al. (2015). Functional system and areal organization of a highly sampled individual human brain. Neuron *87*, 657–670.

Laumann, T.O., Snyder, A.Z., Mitra, A., Gordon, E.M., Gratton, C., Adeyemo, B., Gilmore, A.W., Nelson, S.M., Berg, J.J., Greene, D.J., et al. (2017). On the stability of BOLD fMRI correlations. Cereb. Cortex *27*, 4719–4732.

Lewis, C.M., Baldassarre, A., Committeri, G., Romani, G.L., and Corbetta, M. (2009). Learning sculpts the spontaneous activity of the resting human brain. Proc. Natl. Acad. Sci. USA *106*, 17558–17563.

Liégeois, R., Laumann, T.O., Snyder, A.Z., Zhou, J., and Yeo, B.T.T. (2017). Interpreting temporal fluctuations in resting-state functional connectivity MRI. Neuroimage *163*, 437–455.

Marcus, D.S., Harwell, J., Olsen, T., Hodge, M., Glasser, M.F., Prior, F., Jenkinson, M., Laumann, T., Curtiss, S.W., and Van Essen, D.C. (2011). Informatics and data mining tools and strategies for the human connectome project. Front. Neuroinform. *5*, 4.

McKiernan, K.A., Kaufman, J.N., Kucera-Thompson, J., and Binder, J.R. (2003). A parametric manipulation of factors affecting task-induced deactivation in functional neuroimaging. J. Cogn. Neurosci. *15*, 394–408.

Menon, V. (2011). Large-scale brain networks and psychopathology: a unifying triple network model. Trends Cogn. Sci. *15*, 483–506.

Miezin, F.M., Maccotta, L., Ollinger, J.M., Petersen, S.E., and Buckner, R.L. (2000). Characterizing the hemodynamic response: effects of presentation rate, sampling procedure, and the possibility of ordering brain activity based on relative timing. Neuroimage *11*, 735–759.

Miranda-Dominguez, O., Mills, B.D., Carpenter, S.D., Grant, K.A., Kroenke, C.D., Nigg, J.T., and Fair, D.A. (2014). Connectotyping: model based fingerprinting of the functional connectome. PLoS ONE *9*, e111048.

Mitra, A., and Raichle, M.E. (2016). How networks communicate: propagation patterns in spontaneous brain activity. Philos. Trans. R. Soc. Lond. B Biol. Sci. *371*, 20150546.

Mitra, A., Snyder, A.Z., Tagliazucchi, E., Laufs, H., and Raichle, M.E. (2015). Propagated infra-slow intrinsic brain activity reorganizes across wake and slow wave sleep. eLife *4*, e10781.

Mueller, S., Wang, D., Fox, M.D., Yeo, B.T., Sepulcre, J., Sabuncu, M.R., Shafee, R., Lu, J., and Liu, H. (2013). Individual variability in functional connectivity architecture of the human brain. Neuron *77*, 586–595.

Noble, S., Spann, M.N., Tokoglu, F., Shen, X., Constable, R.T., and Scheinost, D. (2017). Influences on the test-retest reliability of functional connectivity MRI and its relationship with behavioral utility. Cereb. Cortex *27*, 5415–5429.

Ollinger, J.M., Corbetta, M., and Shulman, G.L. (2001). Separating processes within a trial in event-related functional MRI II. Analysis. Neuroimage *13*, 218–229.

Pannunzi, M., Hindriks, R., Bettinardi, R.G., Wenger, E., Lisofsky, N., Martensson, J., Butler, O., Filevich, E., Becker, M., Lochstet, M., et al. (2017). Resting-state fMRI correlations: from link-wise unreliability to whole brain stability. Neuroimage *157*, 250–262.

Pearce, T.M., and Moran, D.W. (2012). Strategy-dependent encoding of planned arm movements in the dorsal premotor cortex. Science *337*, 984–988.

Poldrack, R.A., Laumann, T.O., Koyejo, O., Gregory, B., Hover, A., Chen, M.Y., Gorgolewski, K.J., Luci, J., Joo, S.J., Boyd, R.L., et al. (2015). Long-term neural and physiological phenotyping of a single human. Nat. Commun. *6*, 8885.

Power, J.D., Cohen, A.L., Nelson, S.M., Wig, G.S., Barnes, K.A., Church, J.A., Vogel, A.C., Laumann, T.O., Miezin, F.M., Schlaggar, B.L., and Petersen, S.E. (2011). Functional network organization of the human brain. Neuron *72*, 665–678.

Power, J.D., Barnes, K.A., Snyder, A.Z., Schlaggar, B.L., and Petersen, S.E. (2012). Spurious but systematic correlations in functional connectivity MRI networks arise from subject motion. Neuroimage *59*, 2142–2154.

Power, J.D., Schlaggar, B.L., Lessov-Schlaggar, C.N., and Petersen, S.E. (2013). Evidence for hubs in human functional brain networks. Neuron *79*, 798–813.

Power, J.D., Mitra, A., Laumann, T.O., Snyder, A.Z., Schlaggar, B.L., and Petersen, S.E. (2014). Methods to detect, characterize, and remove motion artifact in resting state fMRI. Neuroimage *84*, 320–341.

Raichle, M.E., MacLeod, A.M., Snyder, A.Z., Powers, W.J., Gusnard, D.A., and Shulman, G.L. (2001). A default mode of brain function. Proc. Natl. Acad. Sci. USA *98*, 676–682.

Righi, G., Peissig, J.J., and Tarr, M.J. (2012). Recognizing disguised faces. Vis. Cogn. *20*, 143–169.

Rosvall, M., and Bergstrom, C.T. (2008). Maps of random walks on complex networks reveal community structure. Proc. Natl. Acad. Sci. USA *105*, 1118–1123.

Satterthwaite, T.D., Wolf, D.H., Erus, G., Ruparel, K., Elliott, M.A., Gennatas, E.D., Hopson, R., Jackson, C., Prabhakaran, K., Bilker, W.B., et al. (2013a).

Functional maturation of the executive system during adolescence. J. Neurosci. *33*, 16249–16261.

Satterthwaite, T.D., Wolf, D.H., Ruparel, K., Erus, G., Elliott, M.A., Eickhoff, S.B., Gennatas, E.D., Jackson, C., Prabhakaran, K., Smith, A., et al. (2013b). Heterogeneous impact of motion on fundamental patterns of developmental changes in functional connectivity during youth. Neuroimage *83*, 45–57.

Sheffield, J.M., and Barch, D.M. (2016). Cognition and resting-state functional connectivity in schizophrenia. Neurosci. Biobehav. Rev. *61*, 108–120.

Shehzad, Z., Kelly, C., Reiss, P.T., Cameron Craddock, R., Emerson, J.W., McMahon, K., Copland, D.A., Castellanos, F.X., and Milham, M.P. (2014). A multivariate distance-based analytic framework for connectome-wide association studies. Neuroimage *93*, 74–94.

Shine, J.M., Bissett, P.G., Bell, P.T., Koyejo, O., Balsters, J.H., Gorgolewski, K.J., Moodie, C.A., and Poldrack, R.A. (2016). The dynamics of functional brain networks: integrated network states during cognitive task performance. Neuron *92*, 544–554.

Shirer, W.R., Ryali, S., Rykhlevskaia, E., Menon, V., and Greicius, M.D. (2012). Decoding subject-driven cognitive states with whole-brain connectivity patterns. Cereb. Cortex *22*, 158–165.

Shulman, G.L., Fiez, J.A., Corbetta, M., Buckner, R.L., Miezin, F.M., Raichle, M.E., and Petersen, S.E. (1997). Common blood flow changes across visual tasks: II. Decreases in cerebral cortex. J. Cogn. Neurosci. *9*, 648–663.

Singh, K.D., and Fawcett, I.P. (2008). Transient and linearly graded deactivation of the human default-mode network by a visual detection task. Neuroimage *41*, 100–112.

Smith, S.M., Jenkinson, M., Woolrich, M.W., Beckmann, C.F., Behrens, T.E., Johansen-Berg, H., Bannister, P.R., De Luca, M., Drobnjak, I., Flitney, D.E., et al. (2004). Advances in functional and structural MR image analysis and implementation as FSL. Neuroimage *23* (*Suppl 1*), S208–S219.

Smith, S.M., Fox, P.T., Miller, K.L., Glahn, D.C., Fox, P.M., Mackay, C.E., Filippini, N., Watkins, K.E., Toro, R., Laird, A.R., and Beckmann, C.F. (2009). Correspondence of the brain's functional architecture during activation and rest. Proc. Natl. Acad. Sci. USA *106*, 13040–13045.

Stam, C.J. (2014). Modern network science of neurological disorders. Nat. Rev. Neurosci. *15*, 683–695.

Tagliazucchi, E., and Laufs, H. (2014). Decoding wakefulness levels from typical fMRI resting-state data reveals reliable drifts between wakefulness and sleep. Neuron *82*, 695–708.

Talairach, J., and Tournoux, P. (1988). Co-planar Stereotaxic Atlas of the Human Brain: 3-Dimensional Proportional System: An Approach to Cerebral Imaging (Georg Thieme).

Tavor, I., Jones, O.P., Mars, R.B., Smith, S.M., Behrens, T.E., and Jbabdi, S. (2016). Task-free MRI predicts individual differences in brain activity during task performance. Science *352*, 216–220.

Van Essen, D.C., Glasser, M.F., Dierker, D.L., Harwell, J., and Coalson, T. (2012). Parcellations and hemispheric asymmetries of human cerebral cortex analyzed on surface-based atlases. Cereb. Cortex *22*, 2241–2262.

Wang, D., Buckner, R.L., Fox, M.D., Holt, D.J., Holmes, A.J., Stoecklein, S., Langs, G., Pan, R., Qian, T., Li, K., et al. (2015). Parcellating cortical functional networks in individuals. Nat. Neurosci. *18*, 1853–1860.

Xie, H., Calhoun, V.D., Gonzalez-Castillo, J., Damaraju, E., Miller, R., Bandettini, P.A., and Mitra, S. (2017). Whole-brain connectivity dynamics reflect both task-specific and individual-specific modulation: a multitask study. Neuroimage. Published online May 23, 2017. https://doi.org/10.1016/j.neuroimage.2017.05.050.

Yeo, B.T., Krienen, F.M., Sepulcre, J., Sabuncu, M.R., Lashkari, D., Hollinshead, M., Roffman, J.L., Smoller, J.W., Zöllei, L., Polimeni, J.R., et al. (2011). The organization of the human cerebral cortex estimated by intrinsic functional connectivity. J. Neurophysiol. *106*, 1125–1165.

STAR★METHODS

KEY RESOURCES TABLE

REAGENT or RESOURCE	SOURCE	IDENTIFIER
Deposited Data		
Raw and processed MRI data	Gordon et al., 2017c	https://openfmri.org/dataset/ds000224 Accession # ds000224
Task fMRI activations	Gordon et al., 2017c	https://neurovault.org/collections/2447/
Psychological Image Collection at Stirling 2D face set		http://pics.psych.stir.ac.uk/
CNBC Tarrlab "Face Place" repository	Righi et al., 2012	http://wiki.cnbc.cmu.edu/Face_Place
Park Aging Mind Laboratory Face Database		http://agingmind.utdallas.edu/download-stimuli/face-database/
Libor Spacek's Facial Imaging Database		http://cmp.felk.cvut.cz/~spacelib/faces/
English Lexicon Project	Balota et al., 2007	http://elexicon.wustl.edu/
Software and Algorithms		
MATLAB	Mathworks	RRID:SCR_001622; https://www.mathworks.com/
Connectome Workbench	Marcus et al., 2011	RRID:SCR_008750; https://www.humanconnectome.org/software/connectome-workbench.html
Freesurfer	Dale et al., 1999	RRID:SCR_001847; https://surfer.nmr.mgh.harvard.edu/
FSL	Smith et al., 2004	RRID:SCR_002823; https://fsl.fmrib.ox.ac.uk/fsl/fslwiki
4dfp tools		ftp://imaging.wustl.edu/pub/raichlab/4dfp_tools/
Freesurfer to fs_LR pipeline	Van Essen et al., 2012	http://brainvis.wustl.edu/wiki/index.php/Main_Page
Parcellation code	Gordon et al., 2016	http://www.nil.wustl.edu/labs/petersen/Resources_files/Surface_parcellation_distribute.zip
Infomap	Rosvall and Bergstrom, 2008	http://www.mapequation.org

CONTACT FOR REAGENT AND RESOURCE SHARING

Further information and requests for resources should be directed to and will be fulfilled by the Lead Contact, Caterina Gratton (cgratton@wustl.edu).

EXPERIMENTAL MODEL AND SUBJECT DETAILS

The publicly available Midnight Scan Club (MSC) dataset was used for analyses (https://openfmri.org/dataset/ds000224/). The dataset and processing has been previously described in detail (Gordon et al., 2017c). We provide an overview of relevant aspects of this dataset and processing below, and then describe specific analyses employed in this manuscript.

Participants and Study Design

The MSC dataset includes structural and functional MRI data as well as behavioral measures from 10 individuals (5 females, ages 24-34), each scanned in 12 separate sessions. Each session occurred on a separate day, beginning at midnight. Daily sessions were conducted in close succession, with the full set of 12 sessions completed within 7 weeks for all participants. Participant MSC08 was excluded from this study due to high levels of head motion and self-reported sleep (Gordon et al., 2017c), leaving nine participants in final analyses. All participants provided written informed consent. Procedures were approved by the Washington University Institutional Review Board and School of Medicine Human Studies Committee.

The first two sessions were used to acquire structural MRI data from each participant. During each of the subsequent 10 sessions, participants completed a functional MRI resting-state scan followed by fMRI scans in four other task states: a motor task, a semantic task, a coherence task, and an incidental encoding memory task. MRI acquisition parameters and tasks are described below.

METHOD DETAILS

MRI Data Acquisition

MRI data were acquired on a 3T Siemens Trio. Structural MRI data collection included multiple T1, T2, MRA, and MRV scans. For the purposes of the current study only the T1 and T2 weighted scans were utilized (for alignment; T1 weighted scans were collected using a MP-RAGE sequence, with TE = 3.74ms, TR = 2.4 s, TI = 1000ms, flip angle = 8°, voxels = isotropic 0.8 mm^3, 224 sagittal slices; T2 weighted scans were collected with TE = 479ms, TR = 3.2 s, voxels = isotropic 0.8 mm^3, 224 sagittal slices).

Functional MRI data were collected using a gradient-echo EPI BOLD sequence (TE = 27ms, TR = 2.2 s, flip angle = 90°, voxels = isotropic 4mm^3, 36 axial slices). The same parameters were used to collect a gradient echo field map acquired during each session for de-warping of the functional data. Participant wakefulness during each scan was monitored with an in scanner eye camera.

Task Designs and Analysis

Functional MRI data were acquired and analyzed for five different conditions, described in detail in Gordon et al. (2017c) and briefly below. Task activations were modeled with a general linear model (GLM; (Miezin et al., 2000)) using in-house software written in IDL (Research Systems, Inc.). All GLMs included baseline and trend regressors, in addition to the regressors specified below. For task functional network analyses, residuals from the GLM analysis were used for time-series correlations, following the ''background connectivity'' approach (Al-Aidroos et al., 2012; Fair et al., 2007).

Resting-state

Each session began with a single 30 min. resting-state scan, during which participants were asked to lie still while fixating on a white cross presented against a black background.

Motor Task

Each session included two runs (7.8 min. total) of a blocked motor task adapted from the Human Connectome Project (Barch et al., 2013). In each block, participants were cued to move either their left or right hand, left or right foot, or tongue. Each block (15.4 s in duration) began with a 2.2 s. cue, followed by a fixation caret flashing every 1.1 s. to signal a movement. Each run included two blocks of each type of movement, as well as three fixation blocks (15.4 s).

In the motor GLM, each motor condition (left hand, right hand, left foot, right foot, tongue) was modeled separately with block regressors convolved with a hemodynamic response function.

Semantic Task

Each session included two runs (14.2 min. total) that each included four blocks, two of the semantic task and two of the coherence task (see below). Both tasks had a mixed block/event-related design, modeled after the tasks in Dubis et al. (2016). During the semantic task, a short cue (2.2 s) indicated the start of a block. Subsequently, 30 individual trials were presented, consisting of words presented for 0.5 s with jittered 1.7-8.3 s intervals. Participants were asked to respond whether the words were nouns or verbs (50% nouns and 50% verbs were included). A cue at the end of the block (2.2 s) indicated the end of the block. Forty-four second fixation periods separated blocks.

Coherence Task

The coherence task followed a similar pattern to the semantic task described above, with start and end cues and the same trial timing. In the coherence task, individual trials consisted of arrays of Glass patterns (Glass, 1969): white dots on a black screen that were varied in how concentrically they were arranged (50% or 0% coherence to a concentric arrangement, displayed with equal frequency). Participants were asked to respond whether dots were arranged concentrically or randomly.

The sematic and coherence tasks were modeled together in a single GLM, with a separate regressor included for the entire block for each task type (a ''semantic'' and ''coherence'' sustained signal, modeled with a square block regressor) as well as the following events: start and end cue in each task, noun and verb trials, 50% coherence and 0% coherence trials. Events were modeled with delta functions for each of 8 separate time-points to model the full time course of responses using an FIR approach (Ollinger et al., 2001).

Memory Task

Each session included 3 runs of an event-related incidental encoding (''memory'') task, with a separate run per stimulus type (face, scenes, and words). Within each run, participants viewed 24 images, repeated 3 times. Individual images were presented for 1.7 s, with jittered 0.5 – 4.9 s intervals. In the face runs, participants were asked to respond whether each face was male or female. In the scene run, participants were asked to respond if scenes were indoor or outdoor. In the words run, participants were asked to respond if words were concrete or abstract.

In the memory GLM, trials were modeled separately based on both the stimulus type and number of repetitions (i.e., face-first repeat, face-second repeat, etc.). Each trial was modeled as above, with delta functions across 8 time-points.

QUANTIFICATION AND STATISTICAL ANALYSES

MRI Data Processing and Surface Registration

MRI data were preprocessed and placed on the surface as described in Gordon et al. (2017c) and with shared code available at https://github.com/MidnightScanClub. The steps are summarized briefly below.

Structural MRI

The high-resolution T1 images were averaged together and used to generate hand-edited cortical surfaces using Freesurfer (Dale et al., 1999) and the resulting surfaces were registered into fs_LR_32k surface space as described in Glasser et al., 2013. Separately, an average native T1-to-Talaraich (Talairach and Tournoux, 1988) volumetric atlas transform was calculated. That transform was applied to the fs_LR_32k surfaces to put them into Talaraich volumetric space.

Functional MRI Pre-processing

All fMRI data first underwent pre-processing (in the volume) to correct for artifacts and align data, including slice-timing correction, frame-to-frame alignment to correct for motion, and intensity normalization to mode 1000. Functional data were then registered to the T2 image, which was registered to the high-resolution T1 anatomical image, which in turn had been previously registered to template space. Finally, functional data underwent distortion correction (see (Gordon et al., 2017c)). Registration, atlas transformation, resampling to 3 mm. isotropic resolution, and distortion correction were all combined and applied in a single transformation step (Smith et al., 2004). Subsequent steps were all completed on the atlas transformed and resampled data.

Task fMRI data were processed in the volume using a GLM, with the approach and regressors described above (*Task Designs and Analysis*). The residuals from this model were used to compute task functional connectivity, in the "background connectivity" approach (Al-Aidroos et al., 2012; Fair et al., 2007), after undergoing the same *Functional Network Processing* as the rest data, described below.

Functional Connectivity Processing

Initial functional connectivity pre-processing steps were taken (in the volume) to reduce the influence of artifacts on functional network data. These steps are described in detail in Gordon et al., 2017c and Power et al., 2014, and include (1) demeaning and de-trending of the data, (2) nuisance regression of signals from white matter, cerebrospinal fluid, and the global signal, (3) removal of high motion frames with framewise displacement (FD) > 0.2mm (see below for additional details) and their interpolation using power-spectral matched data, and (4) bandpass filtering (0.009 Hz to 0.08 Hz). After pre-processing in the volume, cortical functional data were registered to the surface (see *Structural MRI*). Cortical surfaces and volumetric subcortical and cerebellar data were combined into the CIFTI data format from Connectome Workbench (Marcus et al., 2011). Finally, data were smoothed (Gaussian kernel, sigma = 2.55mm), with 2-D geodesic smoothing on the surface and 3-D Euclidean smoothing for subcortical volumetric data.

Motion Censoring and Data Quantity

As noted above, data from high motion frames (FD > 0.2mm) were censored from analysis. FD in two subjects (MSC03, MSC10) included correction for high-frequency motion in the AP direction (low-pass filtered at 0.1 Hz; Gordon et al., 2017c). In addition, short segments of data (< 4 contiguous frames) were removed. Each run was required to have a minimum of 25 good volumes and each session was required to have a minimum 50 volumes total for each task. Task data were limited to the task periods of each run (i.e., removing fixation frames).

The following amounts of data were retained for each task across 10 sessions: (1) Rest – mean of 5999/8180 volumes retained per subject (73%, equivalent to 219 min., with a range of 3429-7667 frames), (2) Motor task – mean of 951/1400 volumes retained per subject (68%, equivalent to 35 min., with a range of 249-1281 frames), (3) Semantic task – mean of 1121/1349 volumes retained per subject (83%, equivalent to 41 min., with a range of 874-1336 frames), (4) Coherence task – mean of 1101/1349 volumes retained per subject (82%, equivalent to 40 min., with a range of 879-1322 frames), and (5) Memory task – mean of 2810/3438 volumes retained per subject (82%, equivalent to 103 min., with a range of 1723-3325 frames). Supplementary analyses were conducted on matched amounts of data from each participant/task/session combination (creating functional network matrices from a restricted 675 frames, or 24.8 min; MSC09 was not included in this analysis due to insufficient data).

Functional Networks

Regions and Systems (Figure 1A)

This study examined functional connectivity among 333 cortical group parcels defined based on boundary-mapping techniques in a large group of independent subjects (Gordon et al., 2016); group ROIs were selected to allow for comparison across individuals. These parcels divide into 12 functional systems: somatomotor (SM), somatomotor lateral (SM-lat), visual (Vis), auditory (Aud), cinguloopercular (CO), salience (Sal), frontoparietal (FP), dorsal attention (DAN), ventral attention (VAN), default mode (DMN), parietal memory (PMN), and retrosplenial (RSP)). Low signal regions that grouped poorly into a system were put in an "unassigned" group. Unassigned regions were excluded from all analyses, with the exception of maps of the distributions of effects across brain regions.

Functional Connectivity (FC)

FC was computed by averaging the BOLD time course within each parcel, after removing censored and interpolated frames, and computing correlations between the time-series of each pair of parcels. Task data were limited to task periods within each run (i.e., excluding fixation periods). FC values were Fisher transformed for normality. FC was represented with a parcel x parcel functional network matrix, sorted by system; values along the diagonal blocks represent within-system correlations, and values in the off-diagonal blocks represent between-system correlations. A separate matrix was created for each individual, task, and two 5 session groups (5 sessions were grouped to increase the reliability of FC – see (Gordon et al., 2017c); session set A included data from sessions 1-5, session set B included data from sessions 6-10). Additional control analyses were done on networks created from matched amounts of data (> 675 volumes, or 24.75 min., evenly sampled from each session) or on 10 separated sessions (see Figure S2).

Analysis Overview

Data-driven approaches

We used a classical multidimensional scaling (MDS) approach to depict how task, individual, and session variance affected the similarity among networks in a data driven fashion, and quantified the variance explained with these approaches with principal component analysis (PCA). MDS places data in multidimensional space based on the similarity (Euclidean distance; correlation-based distances produce similar results) among data points – where in this case a data point represents the linearized upper triangle of a given functional network matrix. Each separate matrix (from a given subject, task, and split-half session) was entered into the classical MDS algorithm (implemented using MATLAB 2012, *cmdscale.m*). Multiple dimensions of the data were explored. The percentage of total variance explained by each dimension was quantified from the eigenvalues (PCA) output from this analysis.

Network similarity

The effects of group, individual, session, and task (as well as their interactions) were directly examined by calculating the similarity among each original functional network matrix (i.e., correlation among the linearized upper triangles), creating a second-order ''similarity'' matrix. Similarities were Fisher transformed for normality. Subsequently, the average similarity was examined for functional network matrices that were (1) from different individuals, tasks, and sessions (''group''), (2) from the same task but different individuals (''task''), (3) from the same subject but different tasks and sessions (''individual''), (4) from the same individual and session but different tasks (''individual & session''), or (5) from the same individual and task but different sessions (''individual & task''). These effects were calculated per subject and effects were compared with one another using paired two-tailed t tests, with p values FDR corrected for the number of comparisons (10 comparisons across every pairing of the 5 conditions). Additionally, Figures S2A and S2B plots each effect type separately per subject and per task. A related approach using multivariate distance-based matrix regression has also recently been proposed for use in comparing functional connectivity of individual vertices (Shehzad et al., 2014).

Normalized Relative Effect Magnitude

The five effect types above were also contrasted by calculating their ''normalized relative effect'' magnitudes. In this procedure, we (i) subtracted the baseline from each effect (symbolized by the red lines in Figure 3B). For the group effect there was no baseline. Task and individual effects were baselined relative to the group to determine how much added similarity these two properties provided relative to network matrices from different individuals and tasks. Individual and session as well as individual and task effects were baselined relative to the similarity of networks from the same individual (''individual'' above). We then (ii) divided each effect by the sum total similarity across all effects after baselining. The same analyses were also conducted on data where a separate matrix was computed for each session (Figures S2C–S2E), and from data matched on number of frames (Figure S2B).

System-level effects

To examine the distribution of effects across the brain, we computed the similarity (correlation) of subcomponents of the full functional network, within and among top-down control systems (CO, FP, DAN, VAN, and Salience) or within and among sensorimotor systems (Visual, SM, SM-lat, Auditory). The same network similarity, average effect, and normalized relative effect magnitude measures were recalculated. Differences in the similarity of each effect type were calculated using paired two-sample t tests, FDR corrected for multiple comparisons across effects.

Parcel-level effects

For a more fine-grained analysis of the distributions, similarity was also calculated per parcel, by taking the similarity of that parcel's full row (all network relationships) across different individuals, sessions, and tasks. Each of the five effect types and their normalized relative effect magnitudes were then calculated per parcel, as described above.

Modeling of single network edges

Finally, a formal model was used to examine the influence of each property on single network edges. Using MATLAB's *anovan.m* function, we calculated a mixed-effects ANOVA for each edge that included categorical factors of individual, task, session, and their interactions to explain variance in the functional correlation of that edge. Individual was modeled as a random effect. We then examined the variance explained (R^2) by the full model, as well as the variance explained from each factor (ω^2, calculated as in Cohen, 1973):

$$\omega^2 = \frac{SS_{effect} - df_{effect} * MS_{error}}{MS_{error} + SS_{total}}$$

Results from each edge are represented in functional network matrices, as well as for each parcel (averaged over edges to that parcel). The F-statistics and FDR-corrected p values for these analyses are also reported in the supplement.

Removal of intrinsic architecture

The influence of intrinsic network architecture on network similarity was examined by subtracting the resting-state matrix from each task functional network matrix (as is done frequently in articles examining task-specific functional connectivity (Betti et al., 2013; Cole et al., 2014; Gratton et al., 2016)). Subsequent to this subtraction, the similarity and effect magnitude measurements were calculated as above, along with the system distributions and single edge models. These were contrasted with the network similarity and modeling values from the original (un-subtracted) functional network matrices from the four tasks (excluding the rest condition to be analogous to the subtraction data).

Evoked signal variability

To contrast the variability of brain networks to the variability of evoked signals from tasks, we calculated the similarity among activation maps from different individuals, tasks, and sessions (computed on the same 5-session groupings, as with FC). Task activations were computed with a GLM, as described in *Task Design and Analysis*. For the purposes of this analysis, the GLM was run on the combined surface-volume CIFTI data, to maximize the precision of activation estimates and best match FC (for previous task functional connectivity purposes, GLMs were run in the volume and residuals were then preprocessed and moved to the surface in order to match the workflow of the resting-state data). Task activations represent the percent signal change in each task for all conditions in that task (against implicit baseline), averaged over vertices within each parcel. The average parcel based task activations from each individual, task, and session-set were then correlated with one another to create a task activation similarity matrix. Each effect type and the normalized relative effect magnitudes were then calculated as above. An ANOVA was also used to calculate the variance explained for the full model and each effect, in this case per parcel. As before, these relative effect sizes were contrasted with the original functional network matrix similarity, excluding the rest condition to best match the task activation analyses.

DATA AND SOFTWARE AVAILABILITY

Raw and preprocessed data associated with this work are available through the Open fMRI data repository at https://openfmri.org/dataset/ds000224/, as detailed in Gordon et al., 2017c. Processing code is available at: https://github.com/MidnightScanClub/MSCcodebase.